

5-17-2012

Correlation of Shear Strength Between Longitudinal and Transverse Specimens

Erasto A. Fernandez

University of New Orleans, efernan2@uno.edu

Recommended Citation

Fernandez, Erasto A., "Correlation of Shear Strength Between Longitudinal and Transverse Specimens" (2012). *University of New Orleans Theses and Dissertations*. Paper 1435.
<http://scholarworks.uno.edu/td/1435>

This Thesis is brought to you for free and open access by the Dissertations and Theses at ScholarWorks@UNO. It has been accepted for inclusion in University of New Orleans Theses and Dissertations by an authorized administrator of ScholarWorks@UNO. The author is solely responsible for ensuring compliance with copyright. For more information, please contact scholarworks@uno.edu.

Report Documentation Page

Form Approved
OMB No. 0704-0188

Public reporting burden for the collection of information is estimated to average 1 hour per response, including the time for reviewing instructions, searching existing data sources, gathering and maintaining the data needed, and completing and reviewing the collection of information. Send comments regarding this burden estimate or any other aspect of this collection of information, including suggestions for reducing this burden, to Washington Headquarters Services, Directorate for Information Operations and Reports, 1215 Jefferson Davis Highway, Suite 1204, Arlington VA 22202-4302. Respondents should be aware that notwithstanding any other provision of law, no person shall be subject to a penalty for failing to comply with a collection of information if it does not display a currently valid OMB control number.

1. REPORT DATE 17 MAY 2012	2. REPORT TYPE	3. DATES COVERED 00-00-2012 to 00-00-2012			
4. TITLE AND SUBTITLE Correlation of Shear Strength Between Longitudinal and Transverse Specimens		5a. CONTRACT NUMBER			
		5b. GRANT NUMBER			
		5c. PROGRAM ELEMENT NUMBER			
6. AUTHOR(S)		5d. PROJECT NUMBER			
		5e. TASK NUMBER			
		5f. WORK UNIT NUMBER			
7. PERFORMING ORGANIZATION NAME(S) AND ADDRESS(ES) University of New Orleans, 2000 Lakeshore Drive, New Orleans, LA, 70148		8. PERFORMING ORGANIZATION REPORT NUMBER			
9. SPONSORING/MONITORING AGENCY NAME(S) AND ADDRESS(ES)		10. SPONSOR/MONITOR'S ACRONYM(S)			
		11. SPONSOR/MONITOR'S REPORT NUMBER(S)			
12. DISTRIBUTION/AVAILABILITY STATEMENT Approved for public release; distribution unlimited					
13. SUPPLEMENTARY NOTES					
14. ABSTRACT In this thesis, new methods for shear strength are proposed and backed up through extensive experimentation, ABAQUS models and data analysis of Titanium welds of three different alloys. The results are compared with those obtained by using the procedure outlined by AWS B4 for calculating Shear Strength in the transverse and longitudinal directions; this equation is widely used by the American Welding Society (AWS) and all those in search of more efficient designs involving welding. It is a well-documented issue that the equation provided by AWS yields a large discrepancy between the values for shear strength of longitudinal and transverse welds.					
15. SUBJECT TERMS					
16. SECURITY CLASSIFICATION OF:			17. LIMITATION OF ABSTRACT Same as Report (SAR)	18. NUMBER OF PAGES 50	19a. NAME OF RESPONSIBLE PERSON
a. REPORT unclassified	b. ABSTRACT unclassified	c. THIS PAGE unclassified			

Correlation of Shear Strength Between Longitudinal and Transverse Specimens

A Thesis

Submitted to the Graduate Faculty of the
University of New Orleans
in partial fulfillment of the
requirements for the degree of

Master of Science
in Naval Architecture and Marine Engineering

by

Erasto Fernandez

B.S., Florida Atlantic University, 2010

May 2012

To my parents
for their love, support and encouragement.

ACKNOWLEDGEMENTS

Being part of this project has showed me a new meaning to being part of something bigger than myself. The Office of Naval Research's Titanium project and the NSRP's over-welding project have reigned above the variety of projects that are worked by this group; a colorful mix of undergrads, master and PhD students, post doctorates, visiting scholars and faculty.

My project, under ONR's titanium project, has involved a great variety of activities from shipyard visits to NASA, from countless hours of computational analysis to operating unique prototype equipment and highly valuable machinery. It has been the most challenging and fulfilling experience in my engineering career and will always be a fond memory and inspiration. For this I thank the Office of Naval Research for making this program a reality.

First, I would like to thank Dr. Pingsha Dong for giving me an opportunity to be part of this team and being a great motivation for personal growth, work ethic and perseverance, and for pushing me to do things I did not know I could and for taking me places I never thought I would find myself in.

I would like to thank also, Lawrence DeCan, for always being a pillar of support when things were rough and for pushing me even further even when I thought I had nothing else to give. Always pushing forward and full of ideas, he has been an inspiration as a superior and a motivation to always see things from multiple points of view.

Alina Shrestha, Chungie Nie and the rest of our great team, I thank you for being available to help even when we are all always busy; for creating a fun, happy and friendly environment in the spaces we all share.

Lastly, I would like to thank my parents for being always there, always aware and always understanding. Their endless love and support has carried me from starting over in a new country to where I am now, and it will always be my greatest source of motivation, my biggest inspiration, and the most humbling gift I will ever receive in my life. Thank you.

TABLE OF CONTENTS

LIST OF FIGURES	v
LIST OF TABLES	vii
I. ABSTRACT	viii
II. INTRODUCTION	1
III. INTRODUCTION TO WELDING	2
A. Weld size and Measuring	2
1. Weld legs	2
2. Weld throat	6
B. AWS equation for Shear Strength	6
C. Fracture path	7
D. UNO Shear Strength Equations	8
1. Longitudinal Shear Strength	8
2. Transverse Shear Strength	10
E. Heat Affected Zone (HAZ)	11
F. Leg Size Variation	12
G. MIG vs. TIG	13
1. TIG (Tungsten inert gas)	13
2. MIG (Metal inert gas)	13
IV. MATERIALS AND SPECIMEN MATRIX	15
A. Titanium Alloys	15
1. Ti-CP (Grade 2):	15
2. Ti-6-4 (Grade 5):	15
3. Ti-4-2.5 (Grade 38):	15
B. Shear Specimen Matrix	15
V. Pre-test preparations	17
A. Dog Bones	17
B. Shear Specimens	19
1. Longitudinal Shear Specimens	20

2.	Transverse Shear Specimens.....	20
VI.	TESTING	22
A.	Dog Bones	22
B.	Shear Specimens	25
VII.	Data Analysis	27
A.	Dog Bones	27
B.	Shear Specimens	29
VIII.	CONCLUSIONS	39
A.	Better Shear Strength correlation	39
B.	Low Shear Strength values for TIG.....	39
C.	Larger welds have lower Shear Strength than smaller welds	39
	WORKS CITED	40
	VITA	41

LIST OF FIGURES

Figure 1	Throat definition for different weld profiles. a = weld throat.....	2
Figure 2	Detail cross-section of a weld	2
Figure 3	MIG titanium weld displays measuring standards	3
Figure 4	TIG titanium weld displays measuring standards.....	3
Figure 5	Digital caliper	4
Figure 6	Weld Leg measuring detail	5
Figure 7	NSRP definition of weld throat	6
Figure 8	Shear Strength values for typical AWS calculations	7
Figure 9	Typical failure angle for Longitudinal welds [7].....	8
Figure 10	Typical failure for Transverse welds [7]	8
Figure 11	Plot showing the non-linear distribution of stress along the length of Longitudinal specimens	9
Figure 12	ABAQUS model of longitudinal Shear Specimen	9
Figure 13	SCF curve-fitting and equation	10
Figure 14	Geometric representation of the Transverse weld profile including forces involved..	11
Figure 15	HAZ shown in this TIG weld macrograph.....	12

Figure 16 TIG welding taking place at Textron Shipyard	13
Figure 17 MIG welding taking place at Textron Shipyard.....	14
Figure 18 Delivered Shear Specimens.....	16
Figure 19 UNO Dog Bone Dimensions	17
Figure 20 Delivered Dog Bones ready for measuring.....	18
Figure 21 ASTM E8 Dog Bone specifications.....	18
Figure 22 A batch of Dog Bones after being pulled to failure	19
Figure 23 Longitudinal specimen after welding.....	20
Figure 24 Longitudinal specimen after machining is completed.....	20
Figure 25 Transverse specimens after welding	21
Figure 26 Transverse specimens after machining	21
Figure 27 Structures Lab at UNO & the MTS machine.	22
Figure 28 MTS Extensometer ready.....	23
Figure 29 Computer interface for the MTS Tensile machine	24
Figure 30 Broken Dog Bone ready for removal from the MTS machine	25
Figure 31 MTS machine during testing	26
Figure 32 Stress-strain curve with 2% shift.....	27
Figure 33 Close-up of Stress-strain curve showing Yield Stress intersection	28
Figure 34 Typical Load-Displacement curves for Longitudinal & Transverse specimens.....	29
Figure 35 Shear strength results for MIG specimens	30
Figure 36 Low shear strength results for TIG specimens.....	30
Figure 37 Typical TIG profile at the weld root shows large gap for lack of penetration	31
Figure 38 Typical MIG profile at the weld root shows much better quality.....	31
Figure 39 Macro image of a typical TIG weld shows location of close-ups.....	31
Figure 40 Improved vales for MIG shear strength.....	32
Figure 41 Improved values for TIG shear strength	32
Figure 42 Typical distribution of a 1/8" TIG weld	33
Figure 43 Typical smaller values for 3/16" welds	33
Figure 44 Typical profiles at the root of larger 3/16" welds.....	34
Figure 45 Better penetration is visible in these smaller 1/8" welds.....	34
Figure 46 A typical display of the Shear Strength values achieved by the AWS formula and the lack of correlation between the specimens.....	35
Figure 47 A typical display of how UNO Shear Strength results do correlate between Longitudinal and Transverse specimens.....	35
Figure 48 Lack of fusion is clearly visible in this weld after fracture has occurred	36
Figure 49 Cold clad is shown in this weld as the base plate separated entirely from the weld material.....	36
Figure 50 Another example of the recurrent lack of penetration	37

Figure 51 An almost vertical disconnection shows a typical cold clad 37

Figure 52 AWS results using after fracture measurements do not correlate between specimens
..... 38

Figure 53 Shear Strength correlation between Longitudinal and Transverse specimens is
achieved with UNO's equations..... 38

LIST OF TABLES

Table 1..... 16

I. ABSTRACT

In this thesis, new methods for shear strength are proposed and backed up through extensive experimentation, ABAQUS models and data analysis of Titanium welds of three different alloys. The results are compared with those obtained by using the procedure outlined by AWS B4 for calculating Shear Strength in the transverse and longitudinal directions; this equation is widely used by the American Welding Society (AWS) and all those in search of more efficient designs involving welding.

It is a well-documented issue that the equation provided by AWS yields a large discrepancy between the values for shear strength of longitudinal and transverse welds.

Key Words: Shear Strength, Titanium, Weld, Welding, TIG, MIG, HAZ, AWS, Stress, Strain.

II. INTRODUCTION

The purpose of this paper is to provide results and conclusions on the comparisons between the standard definition of traction stress based Shear Strength and the new definition proposed by Dr. Dong and Chung Nie from the Laboratory for Welded Structures in the college of Naval Architecture and Marine Engineering at The University of New Orleans (UNO).

The data used in this paper and all of the project's experimentation was done using specimens made out of Titanium in the following alloys: Grade 2 Ti-CP (commercially pure), Grade 5 Ti6Al4V and Grade 38 Ti-425. An extensive study of the materials themselves had to be conducted for this is also an area where very few papers have been published and never before have these amounts of tests been perform on such an unusual material. A secondary purpose within this paper is to show the capabilities of Titanium.

Due to limited literature available for this project, the majority of the referenced material is from Dr. Dong's previous papers and the pending paper from Chung Nie and Dr. Dong.

This project was executed under funding by the Office of Naval Research (ONR). Specimen preparation was done by Textron Marine and Land Systems. Textron, ONR and UNO are part of a team working on the capabilities and the feasibility of using titanium in the ship building industry in the future.

All available specimens for this project were tested by April 2012.

III. INTRODUCTION TO WELDING

A. Weld size and Measuring

1. Weld legs

The vertical and horizontal legs on welds are measured in the same manner, although they are rarely of the same dimensions. This is due to several factors including the human errors involved in a manual process and the effects of gravity as the weld material settles down.

The vertical and horizontal legs of a weld's cross-section go from the root of the weld to the intersections that the lines originating from the root make with the diagonal line that crosses both ends of the weld toes. This diagonal line is to be tangent to the inner curvature of the weld cap when the profile of the weld is concaved; when it is convex, this line will not go any further away from the root than the connection of both weld toes (Figure 1).

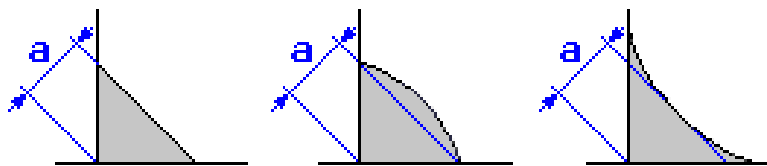


Figure 1 Throat definition for different weld profiles. a = weld throat.

The following image (Figure2) illustrates how the different parts of a weld are broken down:

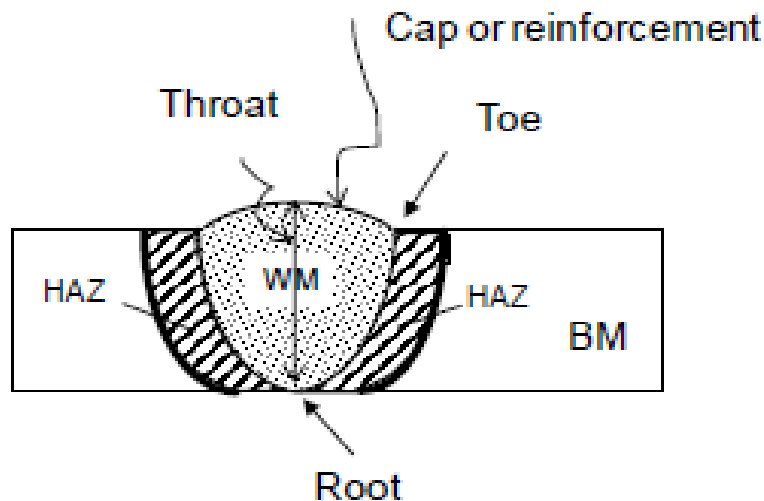


Figure 2 Detail cross-section of a weld

The following are scaled macro pictures of both TIG and MIG titanium welds with their detail measurements marked, they show the difference when it comes to measuring the two different processes used to weld during this project (Figures 3 & 4).



Figure 3 MIG titanium weld displays measuring standards



Figure 4 TIG titanium weld displays measuring standards

Leg sizes were measured both before and after fracture with digital calipers (Figure 5). This long process was carried out six times per weld, including vertical and horizontal legs. All measurements were done at equal distance of each other to acquire the best possible data; since the welds vary in length between transverse and longitudinal shear specimens, the space between the measurements changed to match the weld but always maintaining equal distances between each measurement. This procedure yielded a large amount of data due to the total number of welds in all the specimens in the experiment; a total 3888 weld leg measurements were taken.

In the case of TIG welds, because of the nature of this welding process, the pre-pulled measurements had to be brought down by 1mm to account for the meniscus.

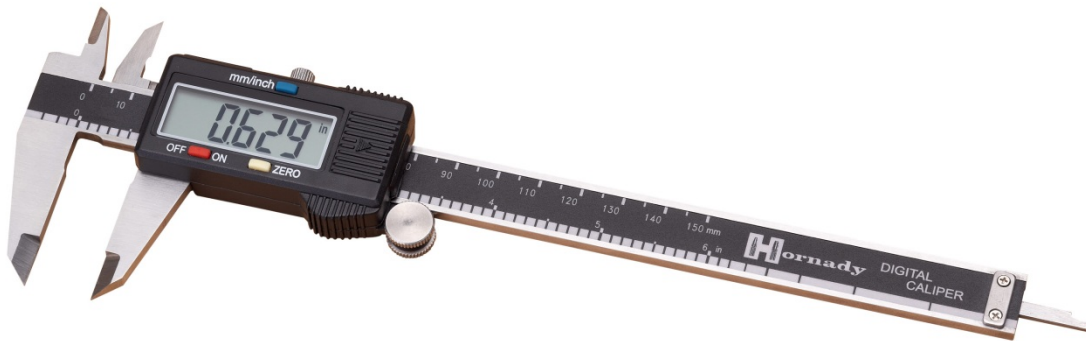


Figure 5 Digital caliper

Figure 6 illustrates how the weld leg measuring process took place along the way. We started by taking the original measurements for X1 and Y1, these values were reduced by the 1mm to account for the meniscus and yielded the new values for X2 and Y2; these are the values used for pre-fracture results.

For the after-fracture results, the value for X3 was measured off the horizontal legs of all broken welds; the X3 values were used in formula (1), derived from similar triangles theory, to scale the Y2 values and yield the Y3 values to complete the after-fracture weld measurements.

$$Y3 = \frac{X3 * Y2}{X2} \quad (1)$$

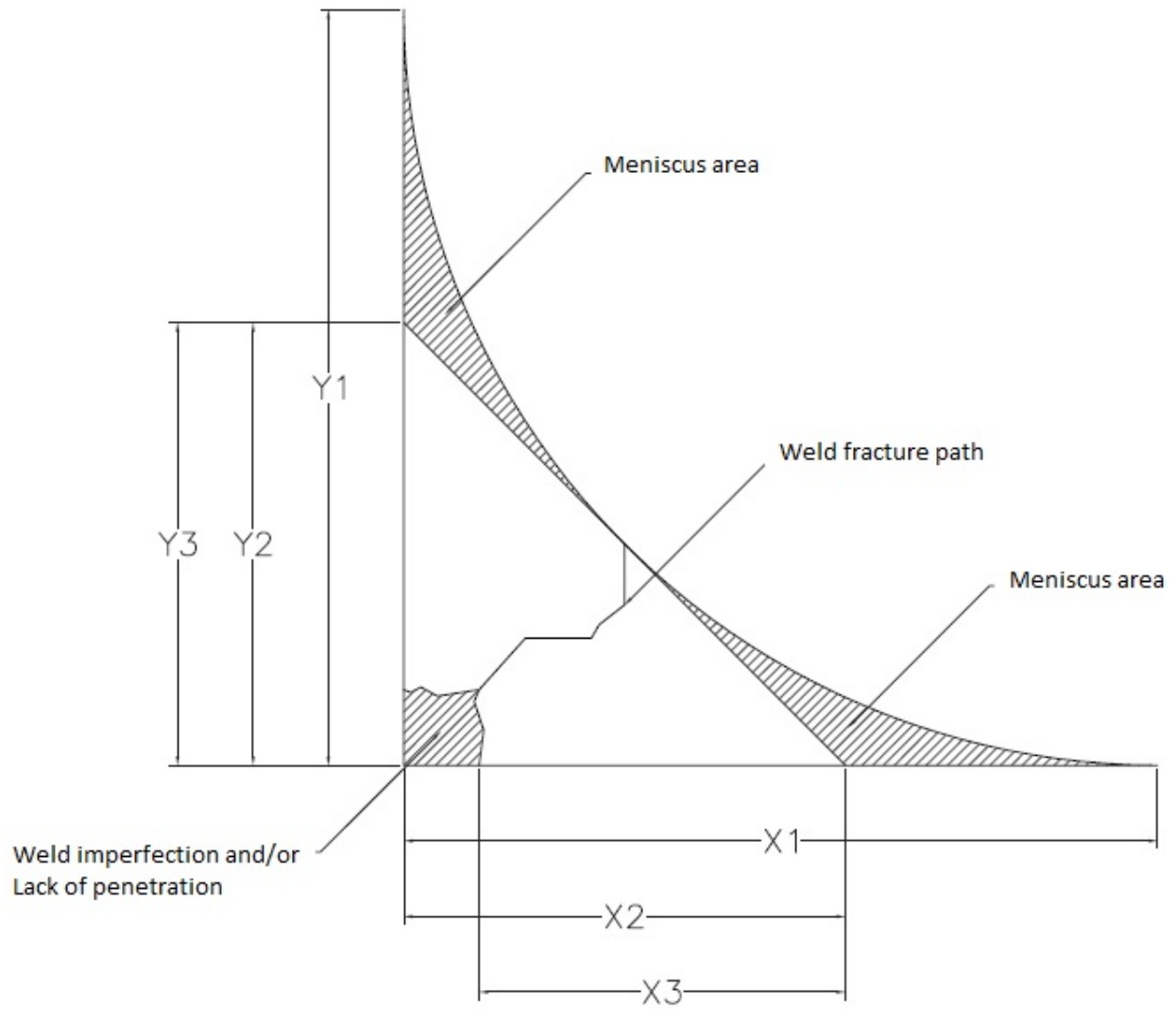


Figure 6 Weld Leg measuring detail

2. Weld throat

The throat of the weld is measured from the root straight to the line joining the weld toes or the tangent of the inner curve of the weld cap (Figure 7); this depends on the weld profile as explained on a previous section of this thesis.

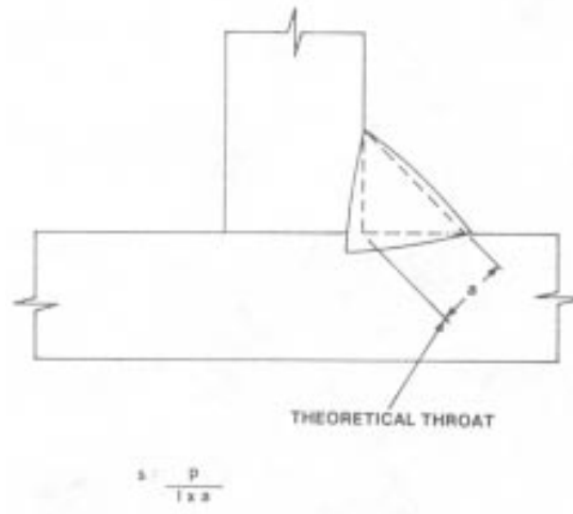


Figure 7 NSRP definition of weld throat

B. AWS equation for Shear Strength

The AWS formula for calculating Shear Strength has been around for quite a while and it is known that it yields values for longitudinal and transverse loads with a large difference between them (Figure 8); There have been other publications that present far more detailed studies explaining the reasons for this behavior, such as the works from Kato and Marta [9] and Timoshenko [8]. This thesis works to provide support of new equations being proposed by members of this team [4] and to prove that they achieve a much higher level of correlation between shear strength in longitudinal and transverse specimens.

The AWS formula for Shear Strength is as follows:

$$\tau_u = \frac{F_u}{a*L} \quad (2)$$

As it is mentioned before, this formula produces results with a large discrepancy between longitudinal and transverse Shear Strength values, this is due in part to the assumption that all welds fracture at 45° from the root; it is a well-documented observation that transverse welds fracture at an angle of approximately 22.5°, making this a different enough process to require other considerations [4].

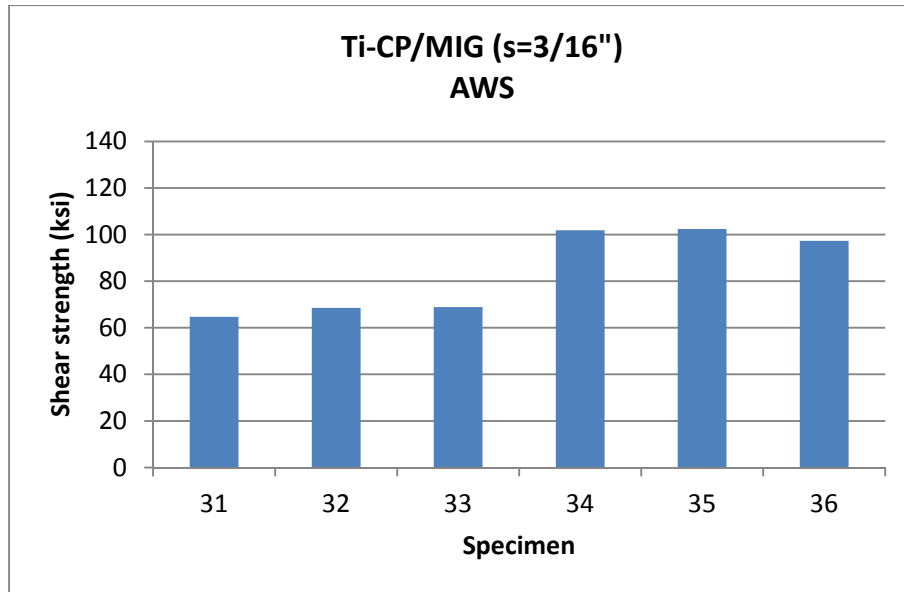


Figure 8 Shear Strength values for typical AWS calculations

Furthermore, the stresses in transverse welds when put under load, have a linear distribution along the length of the weld, contrary to the nonlinear distribution present in longitudinal welds along the same path; this also indicates the need for specific formulations and procedures for each of the two situations. A much more detailed account for these matters is explained in Nie and Dong’s work [4].

C. Fracture path

The welds will fracture along different paths depending if they are Longitudinal or transverse specimens to be tested.

The weld fracture in Longitudinal Shear specimens will follow its path approximately along 45°, originating at the weld root and making its way to the tangent line; this happens due to shear forces acting in opposite directions parallel to the weld length [10], furthermore, the smallest area within the weld along its length is present at an angle of 45° originating from the root.

This path is shown on the following picture in the cross-section of a tested longitudinal specimen (Figure 9):

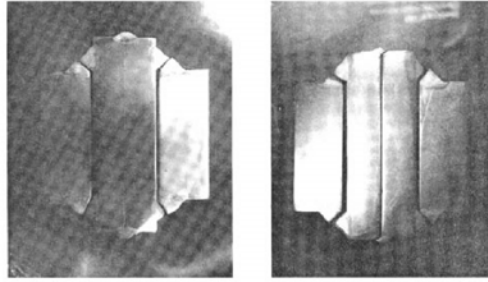


Figure 9 Typical failure angle for Longitudinal welds [7]

The weld fracture in Transverse Shear specimens will follow its path approximately along 22.5° , originating at the weld root and making its way to the tangent line. The following picture shows the path of fracture in a transverse specimen (Figure 10):

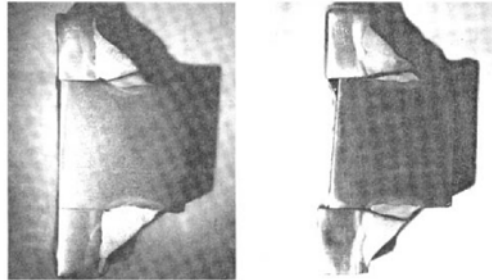


Figure 10 Typical failure for Transverse welds [7]

D. UNO Shear Strength Equations

1. Longitudinal Shear Strength

As mentioned before, stress is not linearly uniform along the length of longitudinal welds, therefore, FEA models (Figure 12) are required to plot the distribution of stress and identify the ultimate stress when the weld fails (Figure 11). Finding this value is critical for the calculation of the Stress Concentration Factor or SCF, a crucial part of the equation.

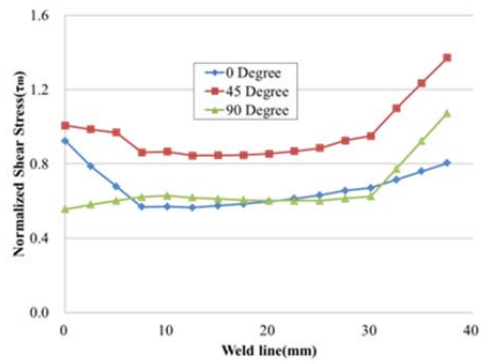


Figure 11 Plot showing the non-linear distribution of stress along the length of Longitudinal specimens

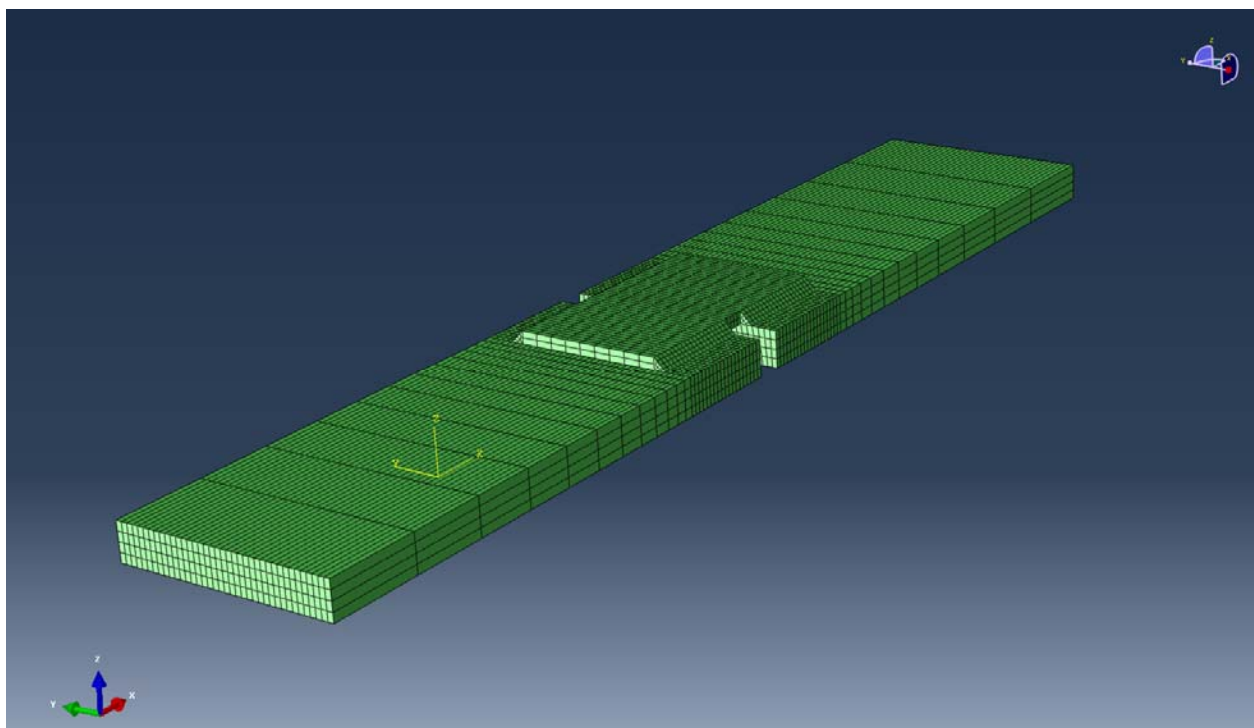


Figure 12 ABAQUS model of longitudinal Shear Specimen

The SCF is defined as the maximum stress value divided by the average stress along the weld length.

$$SCF = \frac{\tau_u}{\frac{F_u}{a \cdot L}} \quad (3)$$

τ_u = Maximum stress value provided by the FEA model's stress distribution curve

F_u = Load applied to specimen [lbs]

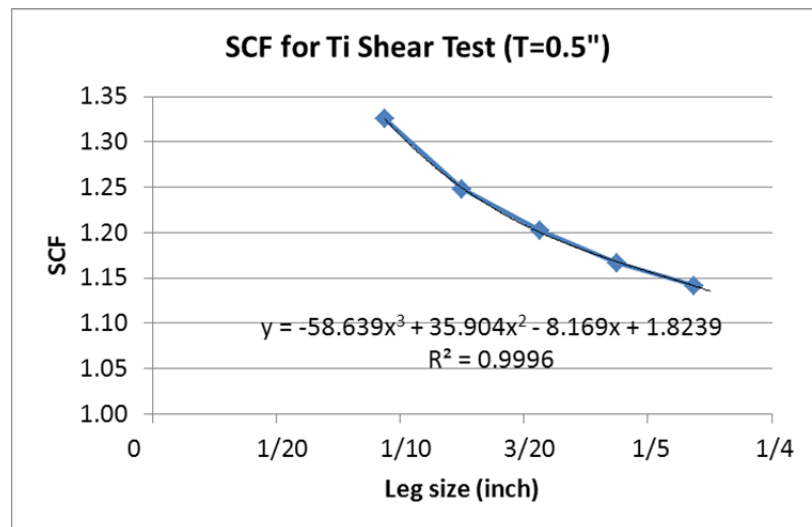
$a = \text{Weld throat at } 45^\circ[\text{in}]$

$L = \text{Total weld length [in]}$

Solving equation (2) for τ_{max} provides the UNO equation for Longitudinal Shear Strength:

$$\tau_u = \frac{SCF * F_u}{a * L} \quad (4)$$

During the process of this project, several models were created and their respective SCF values were used for curve-fitting and obtaining the following equation that allows us to find a specimen's SCF without having to create new models for each one; the curve and equation provided here apply only to the specific design of our specimens.



(5)

Figure 13 SCF curve-fitting and equation

2. Transverse Shear Strength

Extensive detail and precise description of the derivations and procedures relevant to this equation are available in the literature referenced throughout this thesis [4].

The UNO equation governing Transverse welds is derived from the geometrical nature of the weld (Figure 14).

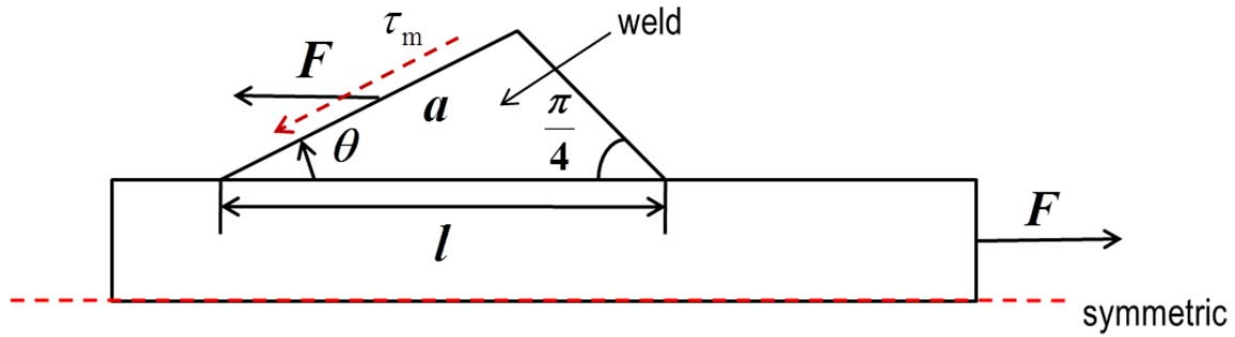


Figure 14 Geometric representation of the Transverse weld profile including forces involved

Equation (5) is the resulting formula for Shear Strength provides a tool that assumes a failure angle of 22.5° and yields proper correlation with its counterpart longitudinal shear strength.

$$\tau_u = \frac{0.854 * F_u}{a * L} \quad (6)$$

E. Heat Affected Zone (HAZ)

The HAZ is the volume of base metal that has been affected during the welding process to the point of altering its microstructure and properties. This volume is clearly depicted in Figure 2 in this thesis.

The extend of these effects causing the HAZ may vary due to different factors such as weld and filler material, amount of heat put in during the process and how concentrated this heat is along the specimen. These effects are shown in the following TIG weld where it can be easily seen how the microstructure changes beyond the point where weld filler material and base metal mix (Figure 15).



Figure 15 HAZ shown in this TIG weld macrograph

F. Leg Size Variation

Welding during this project was done completely by hand and it relied entirely on the welder's abilities and expertise. The welder, knowing the target size, had to picture the size as he laid the weld down; this makes the welding process very subjective and dependent on the welder's correct knowledge and definition of the sizes required. While the welder might be hitting his target to very high level of accuracy, if his mental target is not exactly the same as the real dimension the design requires then the weld will be constantly off from the mark.

We want to obtain the smallest possible weld that we can prove sufficient for the structure at hand, for this the welder has to be able to consistently lay accurate welds at the desired target size.



G. MIG vs. TIG

1. TIG (Tungsten inert gas)

This process involves precise coordination from the welder as he manipulates the torch, the rod of weld filler and the pedal controlling the torch. Due to the nature of this process, it is the slower of the two, therefore, inputting the highest amount of heat into the material causing higher stresses and distortions. TIG welds have a distinctive look: overlapping circles and a concaved in weld profile (Figure 16).

TIG welding done during the weld characterization portion of this project yielded a standard deviation of $0.5/64''$; this is the lower of the two processes and it's due to how controlled and slow TIG welding is compared to MIG. TIG welding also averaged a rate of travel of 3.5 min/ft. making it the slower of the two processes by a large difference (Figure 16).



Figure 16 TIG welding taking place at Textron Shipyard

2. MIG (Metal inert gas)

Metal Inert Gas or as it is most commonly known MIG welding is a much more aggressive and fast process than TIG welding. It averaged a travel rate of 13 sec/ft. making it much faster and therefore, achieving a higher standard deviation of $1.45/64''$. The higher deviation can be attributed to the welder since would have to maintain the same balance and accuracy during a much faster process (Figure 17).

MIG weld are much more common than TIG thanks to the speed they provide. They produce concaved outwards weld profile with minor definition between the weld material (Figure 17).



Figure 17 MIG welding taking place at Textron Shipyard

IV. MATERIALS AND SPECIMEN MATRIX

A. Titanium Alloys

1. Ti-CP (Grade 2):

Titanium “CP” or commercially pure, is unalloyed and in this case is of grade 2. Commercially pure titanium varies from grades 1 to 4, as the grade increases so does the tensile and yield strength of the metal. These variations occur between the four grades due to the different percentages of interstitial elements or “impurities” in the different metals.

2. Ti-6-4 (Grade 5):

Grade 5 titanium is the most commonly used of all the alloys present in this project, it is also known as Ti6AL4V, Ti-6AL-4V and as referred within this team: Ti-6-4. The popularity of this particular alloy is due to it being heat treatable and stronger than CP while retaining most of the thermal properties.

The alloy’s chemical composition is formed by 6% aluminum, 4% vanadium, a maximum of 0.25% iron, a maximum of 0.25% oxygen and the balance in titanium [6].

3. Ti-4-2.5 (Grade 38):

Grade 38’s composition is formed by 4% aluminum, 2.5% vanadium, 1.5% iron and the balance in titanium. This alloy was created by Allegheny Technologies Incorporated (ATI) and they were the sole providers of this metal during this project. ATI called the alloy: ATI 425; it is very similar in its properties to Grade 5 yet it has much better cold workability like other “weaker” alloys [5].

B. Shear Specimen Matrix

The test specimen matrix (Table 1) shows all the specimens that were required by the project and tested by April 2012. These specimens were made of the previously mentioned materials; each different material was used in eight sets of three specimens. These eight sets differed in weld direction (longitudinal or transverse), Weld target size (1/8” or 3/16”) and the welding process used (TIG or MIG).

All specimens were fabricated by Textron and delivered to the laboratory at UNO (Figure 18).

Table 1

REQUIRED NUMBER OF SAMPLES				
	1/8" Weld Size Longitudinal Weld	1/8" Weld Size Transverse Weld	3/16" Weld Size Longitudinal Weld	3/16" Weld Size Transverse Weld
Tig CP GR-2	3	3	3	3
Tig 6-4 GR-5	3	3	3	3
Tig 425 GR-38	3	3	3	3
Mig CP GR-2	3	3	3	3
Mig 6-4 GR-5	3	3	3	3
Mig 425 GR-38	3	3	3	3
Column Total	18	18	18	18
Total Welded Specimen				72



Figure 18 Delivered Shear Specimens

V. Pre-test preparations

A. Dog Bones

The specimens referred to as “dog bones” were designed (Figure 19) by the UNO team and up to the specifications set by the American Society for Testing and Materials in their standard for Tension Testing of Metallic Materials ASTM E8 [1] (Figure 21). These specimens were tested to establish basic material properties of the alloys used in the Titanium project; although this data was used in this project, it has served other projects under the mantle of the Titanium project as well.

The Dog Bones were cutout by Textron Marine and Land System at their shipyard; they were delivered to UNO for inspection, testing and analysis.

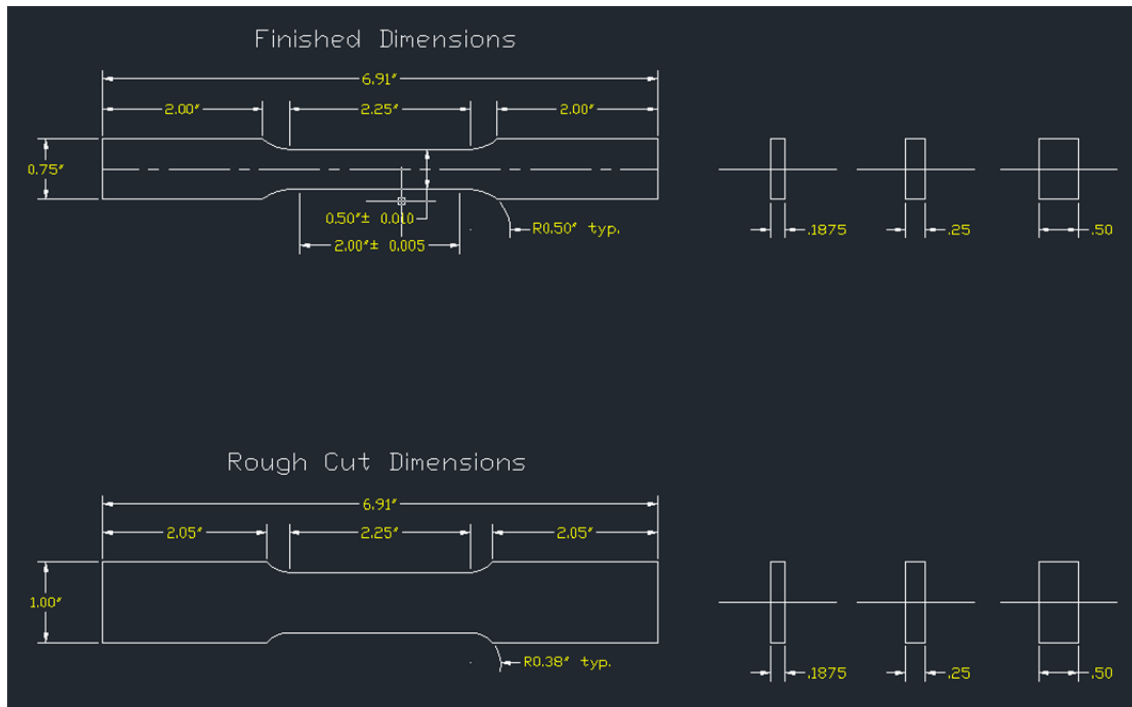


Figure 19 UNO Dog Bone Dimensions

All Dog Bones were separated into their respective groups of three specimens (Figure 20) and then measured individually for width at the grip sections, width at the gage section, thickness throughout the entire specimen, and total length; as indicated in the ASTM E8 [1] (Figure 21) standard's procedure. Several measurements were taken for each location and then averaged for a more accurate analysis.



Figure 20 Delivered Dog Bones ready for measuring

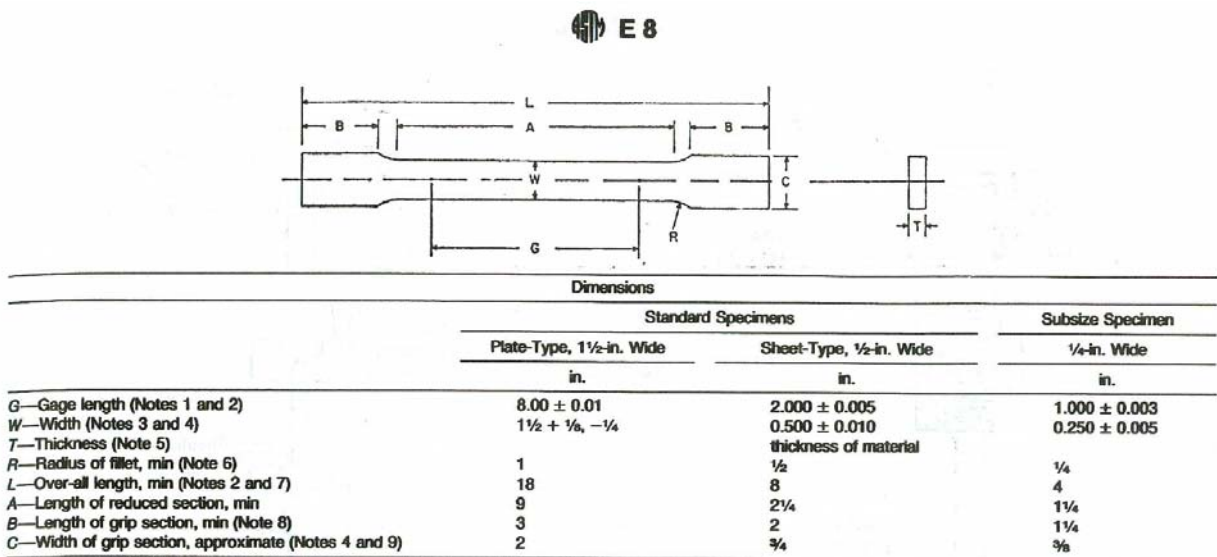


Figure 21 ASTM E8 Dog Bone specifications

For future reference of this project and the specimens tested, all measurements were saved along with pictures of each individual specimen before and after testing (Figure 22).



Figure 22 A batch of Dog Bones after being pulled to failure

B. Shear Specimens

All shear specimens were delivered together to UNO, at this point the team began to prepare all 72 specimens for testing; this involved similar but not identical procedure for both longitudinal and transverse pieces.

All specimens were marked on all four major plates in case any of them separated from the main body after failure. All welds were numbered on each specimen for further tracking of the failure process.

All welds were measured before the specimens were pulled. The measuring techniques are explained with further detail on the corresponding section of this thesis.

Shear specimens were designed as close as possible to meet the ASTM E8 standard [2]; the weld length on the titanium samples had to be shorten so that they would be able to be pulled at UNO due to limitations with the MTS machine.

1. Longitudinal Shear Specimens

Longitudinal specimens had to be sent out for machining once assembly was complete; this machining removed the starts and stops of the welds and allows for a more constant and precise weld without the variations corresponding to the beginning and end processes involved in welding. The following images (Figure 23 & 24) show the longitudinal specimens and how the machining should be done.

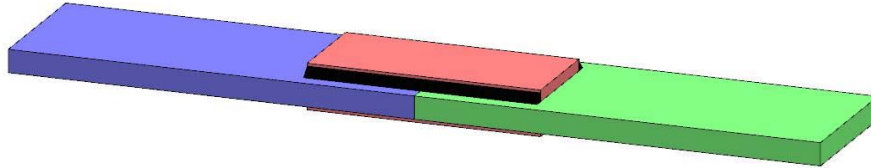


Figure 23 Longitudinal specimen after welding

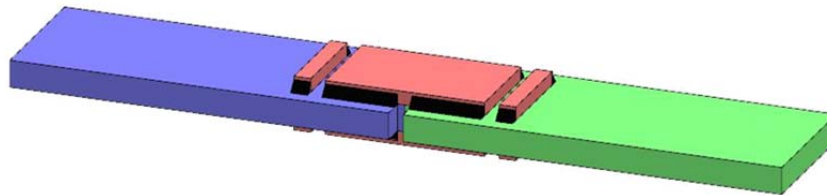


Figure 24 Longitudinal specimen after machining is completed

2. Transverse Shear Specimens

Transverse specimens did not need any modifications after they arrived at UNO's lab and were the first to be measured, marked and photographed. Although the measuring procedure was the same between longitudinal and transverse specimens, the transverse have half the welds by design and were therefore a much faster process.

On the contraire to the longitudinal specimens, the transverse were welded in sets of four and then cut apart from each other and having the ends machined off, this achieved the same result of isolating the welds as the machining necessary on the longitudinal specimens after their arrival.

The following images (Figure 25 & 26) show the transverse specimens during the manufacturing process.

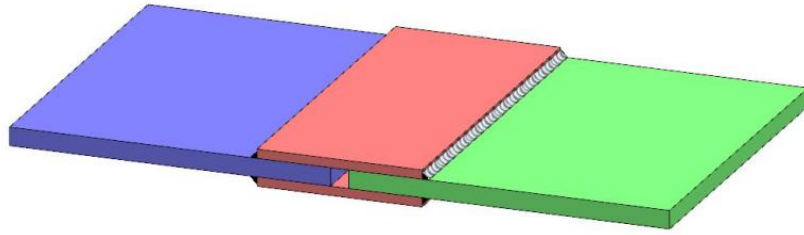


Figure 25 Transverse specimens after welding

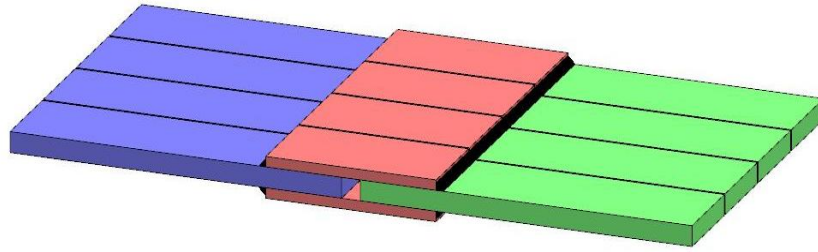


Figure 26 Transverse specimens after machining

VI. TESTING

Specimens for this project were divided in two major groups, one being the Dog Bones for base material property analysis and the other being the shear test specimens for establishing a better correlation between the longitudinal and transverse shear values.

A. Dog Bones

The Dog Bones were tested one by one on the MTS tensile machine in the Structures Laboratory at The University of New Orleans (Figure 27). The procedure that was programmed into the machine's computer was designed up to the same standards that govern the entire test [2]; this allowed to a slow initial pull until the specimen was just pass its yield point, after that point the pulling rate increased automatically and continued at the new rate until failure of the specimen; at this point the machine stopped and reset itself for a new specimen to be mounted (Figure 30).



Figure 27 Structures Lab at UNO & the MTS machine.

Using the metal stoppers provided by MTS the specimens were set centered within the wedges; the same area was gripped at both ends of all specimens. An extensometer (Figure 28), also by MTS, was used to measure the elongation of the specimens to a higher degree of accuracy than the values given by the machine. The extensometer was positioned carefully within the gage length of the Dog Bones after they were set on the machine ready to be pulled.



Figure 28 MTS Extensometer ready

Once the data showed that the specimen had passed the point of yield (Figure 33), the test was paused automatically and the extensometer removed to avoid any damage at the point of failure. The test was resumed once the instrument was off the specimen and the operator was cleared and in a safe location.

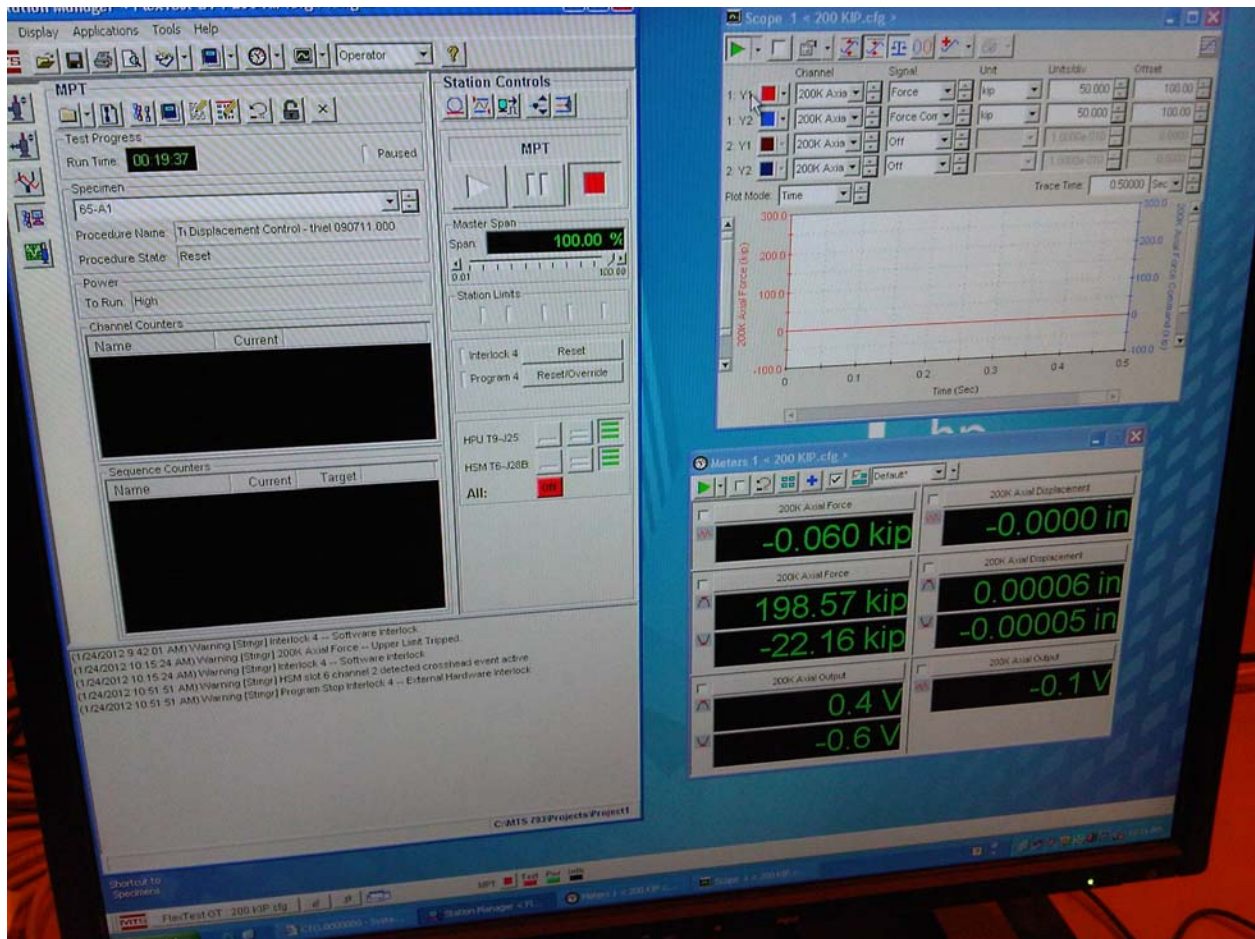


Figure 29 Computer interface for the MTS Tensile machine

After the specimen was successfully pulled (Figure 30) and the data recorded, the pieces were removed from the wedges and stored; the machine was checked for any possible consequences of the recurring testing and then the process continued with each one of the Dog Bones.



Figure 30 Broken Dog Bone ready for removal from the MTS machine

B. Shear Specimens

The procedure for testing the Shear Specimens was also based on ASTM E8 standard [2]; with the exception of the use of the extensometer and without any change in pulling rate, the shear tests were performed in a similar fashion to the procedure previously mentioned for the Dog Bones. Once the specimens were completely processed (measured, marked and photographed), and the machine was prepped for the tests, the specimens were pulled to failure one by one.

Due mostly to the Transverse specimens, special security measures had to be taken because of the high forces involved and the explosive nature of Titanium at the point of failure. Safety was paramount throughout this entire project and all necessary measures were met or exceeded in all working areas.

As predicted, many of the Transverse specimens separated into up to four pieces as a result of all four welds breaking at the point of failure. After all specimens were tested, the broken

horizontal legs were re-measured using the digital calipers (Figure 5); these after-failure horizontal values for leg size were used with the theory of similar triangles [12] to scale the measured before-failure vertical legs while preserving the geometry of the welds. This new measured after-failure data was compared alongside the target weld sizes; this process was carried out for the results to take into account all imperfections contained within the welds (Figure 37).



Figure 31 MTS machine during testing

VII. Data Analysis

A. Dog Bones

As mentioned previously, the sole purpose of the Dog Bone experiments was to determine and corroborate base material properties and so aid the process of proving UNO's equations for correlating Shear Strength. When such an aid was necessary, Stress-strain graphs such Figures 32 & 33 were produced to find Yield and Ultimate strengths of the material in question.

Detailed explanation of this procedure is thoroughly explained by Dr. Dong in his publication [11].

The 2% shift mentioned in Dr. Dong's work is used in Figure 32 & 33 to find the Yield Strength of the material; this is detailed on Figure 33 with a close-up of Figure 32.

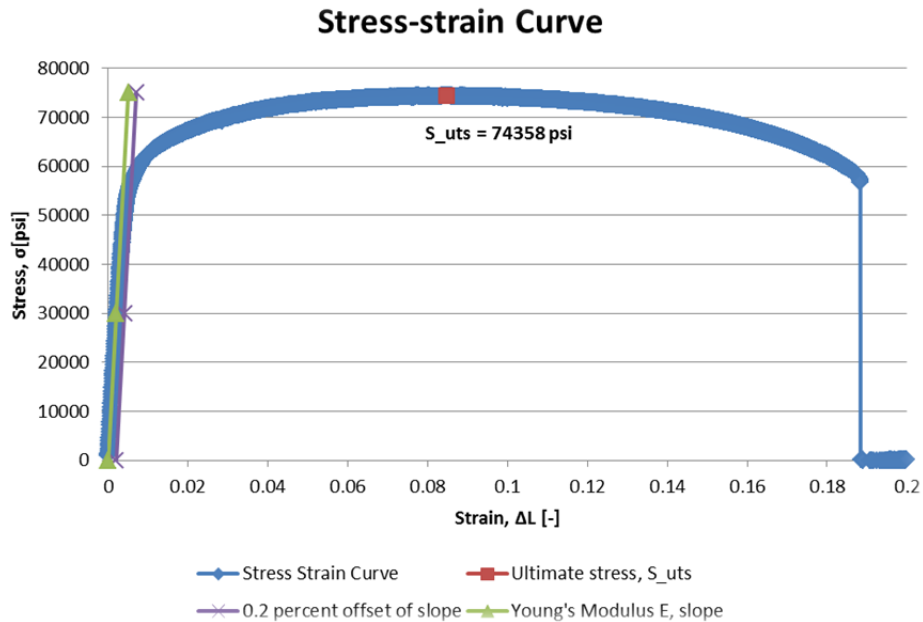


Figure 32 Stress-strain curve with 2% shift

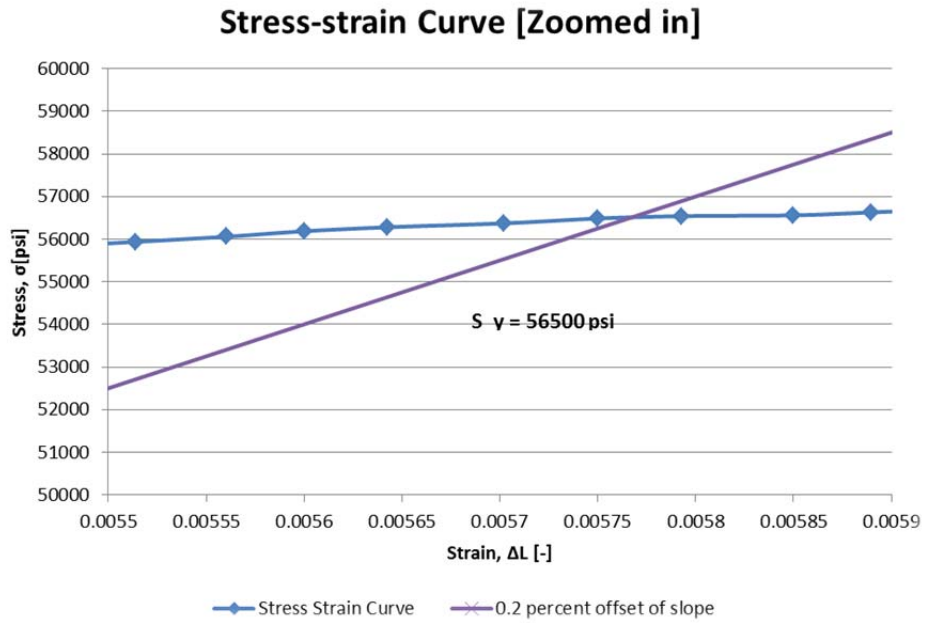


Figure 33 Close-up of Stress-strain curve showing Yield Stress intersection

B. Shear Specimens

A vast amount of data was collected from the 72 titanium shear specimens tested; questions and interesting facts were abundant as the data was revised.

Figure 34 shows the typical profiles that load-displacement curves have for both Longitudinal and Transverse specimens.

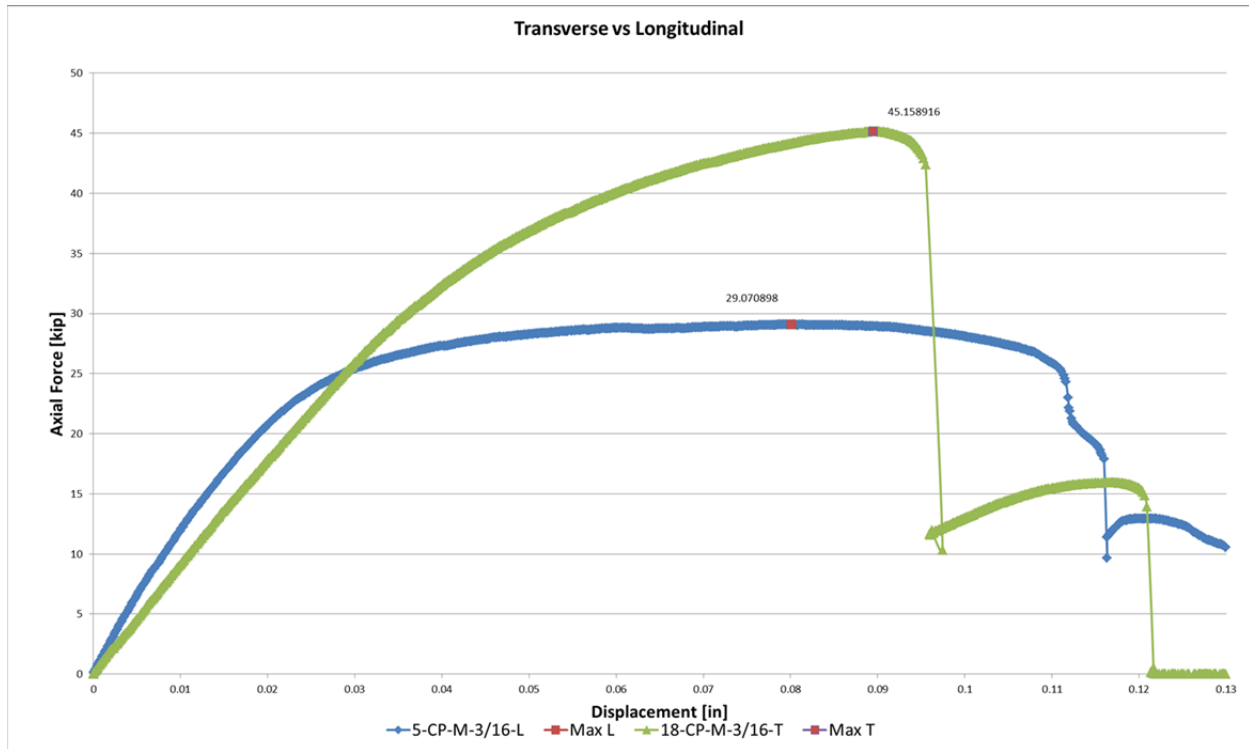


Figure 34 Typical Load-Displacement curves for Longitudinal & Transverse specimens

Two major issues were observed during the analysis process, these are believed to explain some of the misrepresenting data found in the later stages of the project. Values for Shear Strength were found to be distinctively lower in various batches of TIG welded specimens than those of MIG welded samples where both sets are targeted at the same leg size. Also, values for Shear Strength of welds targeted at larger sizes were found to be smaller than those targeted at smaller leg sizes while they both were of the same weld procedure and material.

These two phenomena are believed to be caused mostly due to a higher concentration of weld imperfections in TIG welded samples and in larger leg size welds. The following charts (Figures 35 & 36) showcase the discrepancies found between TIG and MIG welded specimens manufactured to the same leg size and with the same materials:

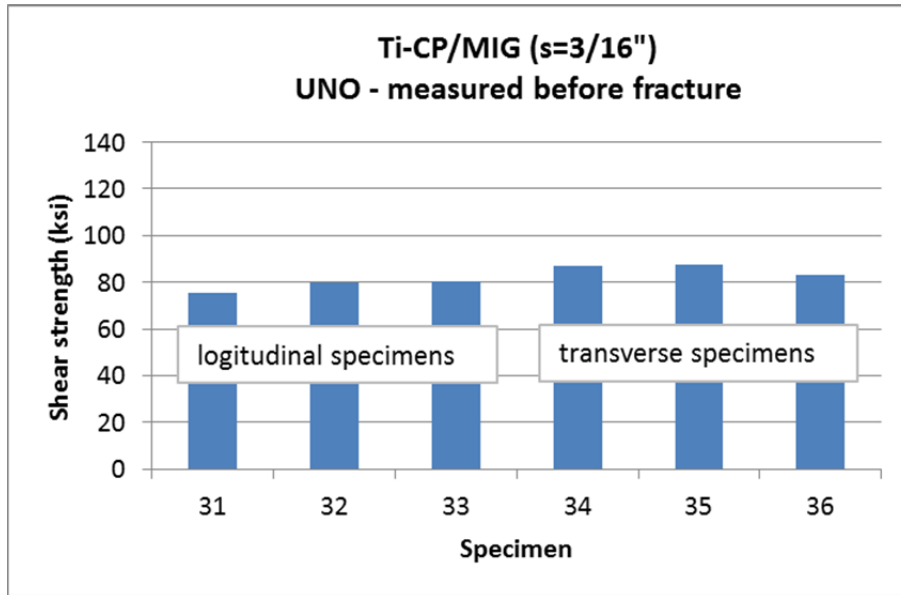


Figure 35 Shear strength results for MIG specimens

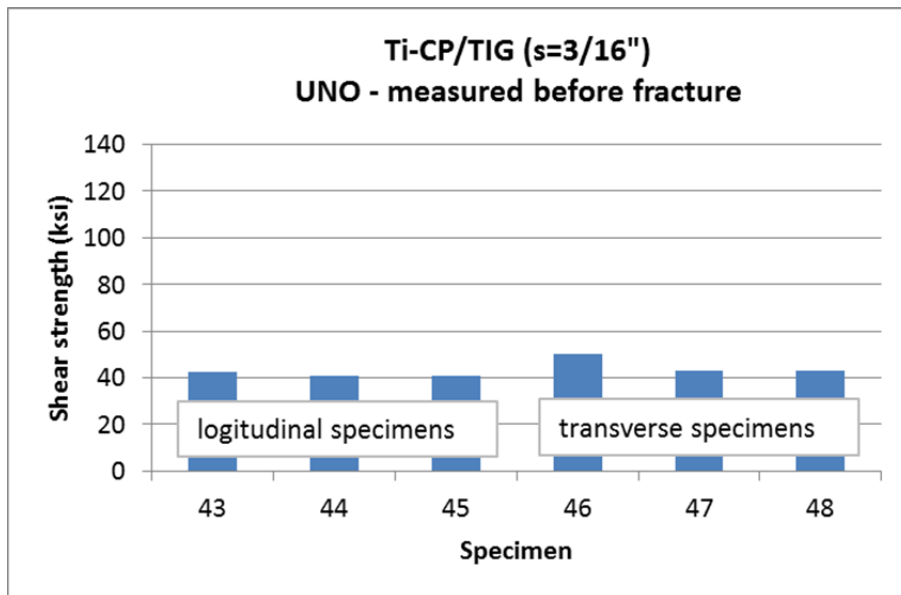


Figure 36 Low shear strength results for TIG specimens

These charts show the consistent discrepancies found in some of the batches of specimens used in this project. Figures 37 & 38 show the typical difference in the weld profiles between TIG and MIG and how TIG welds suffer a higher concentration of imperfections within the welds such as “cold clad” and lack of optimal penetration; they are close-ups of TIG welds in the manner showed in Figure 39.

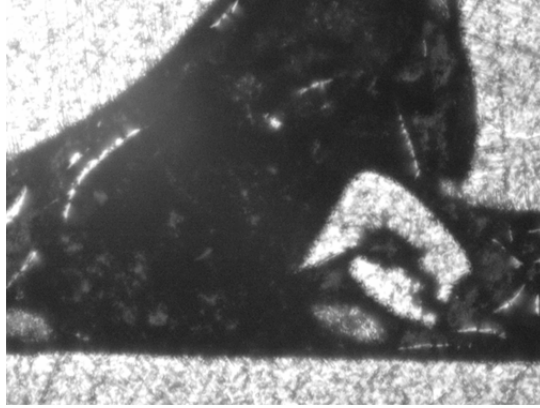


Figure 37 Typical TIG profile at the weld root shows large gap for lack of penetration

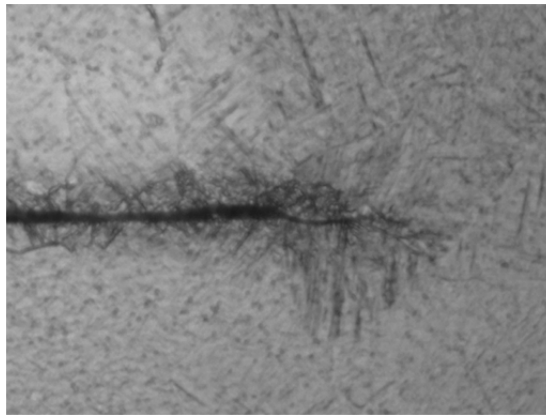


Figure 38 Typical MIG profile at the weld root shows much better quality

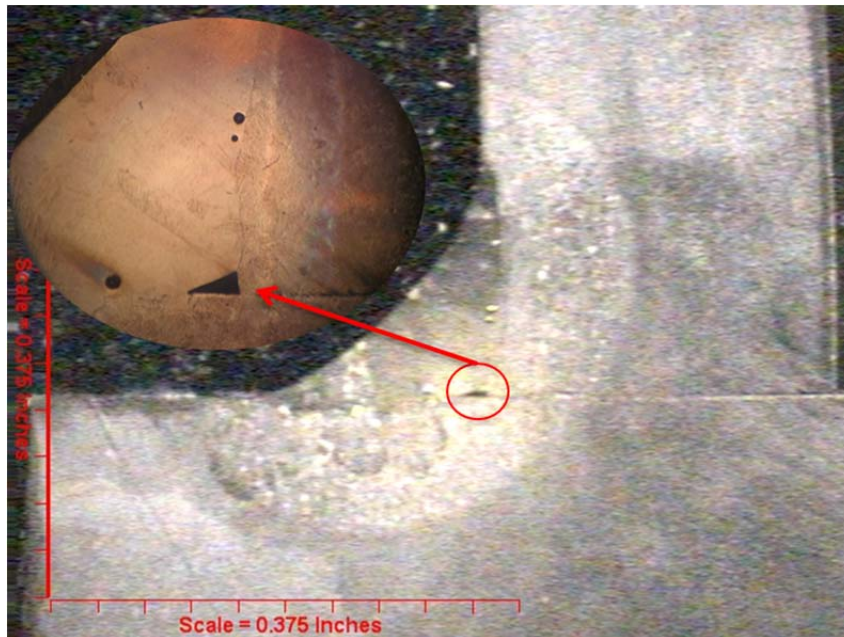


Figure 39 Macro image of a typical TIG weld shows location of close-ups

After considering these irregularities between the different size welds, we took them into account and used the after-fracture measurements. As shown in Figures 40 & 41, the ratio between MIG and TIG shear strengths improved approximately 20% by using the more accurate after-fracture weld leg sizes; although this is an improvement, it does not reconcile the differences between the two welding processes entirely, this might be due to other issues present in the specimens used in this project and they should be investigated further in future research.

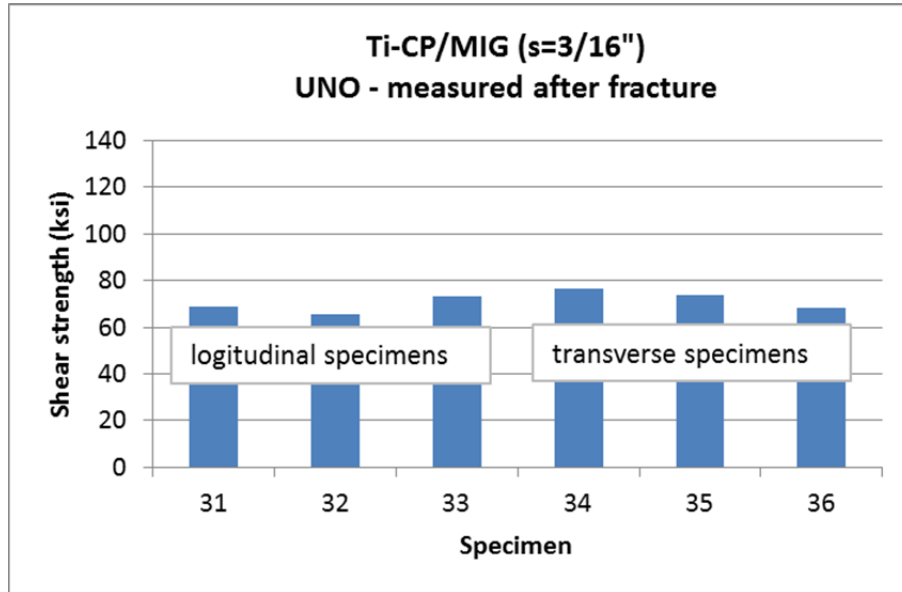


Figure 40 Improved values for MIG shear strength

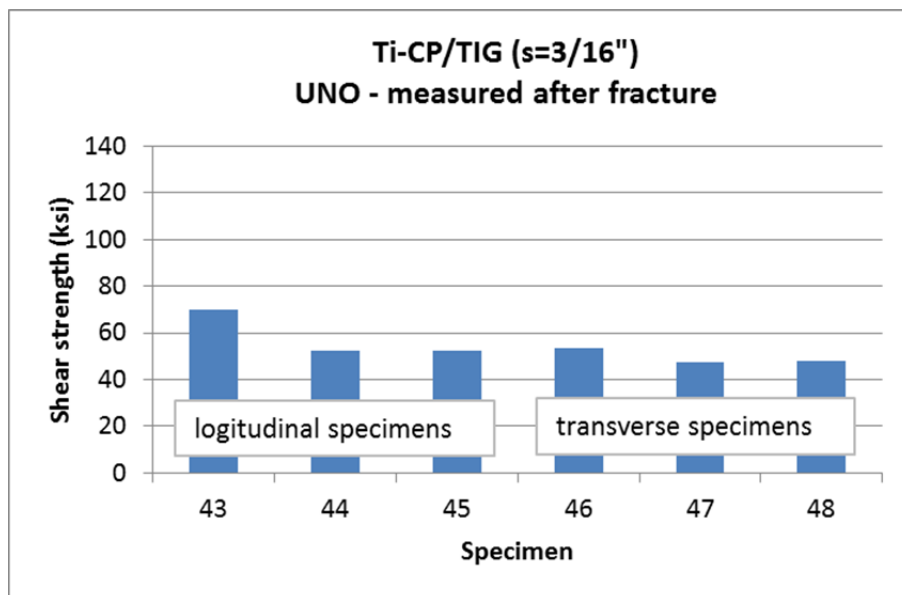


Figure 41 Improved values for TIG shear strength

The following charts show the irregularities between large and small targeted leg size specimens and how those intended to be larger failed at lower loads (Figures 42 & 43).

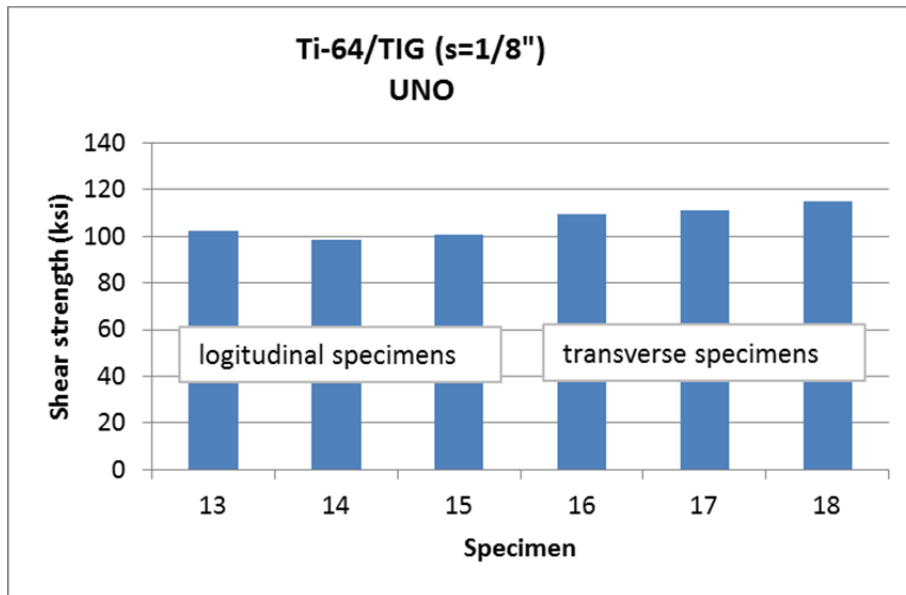


Figure 42 Typical distribution of a 1/8" TIG weld

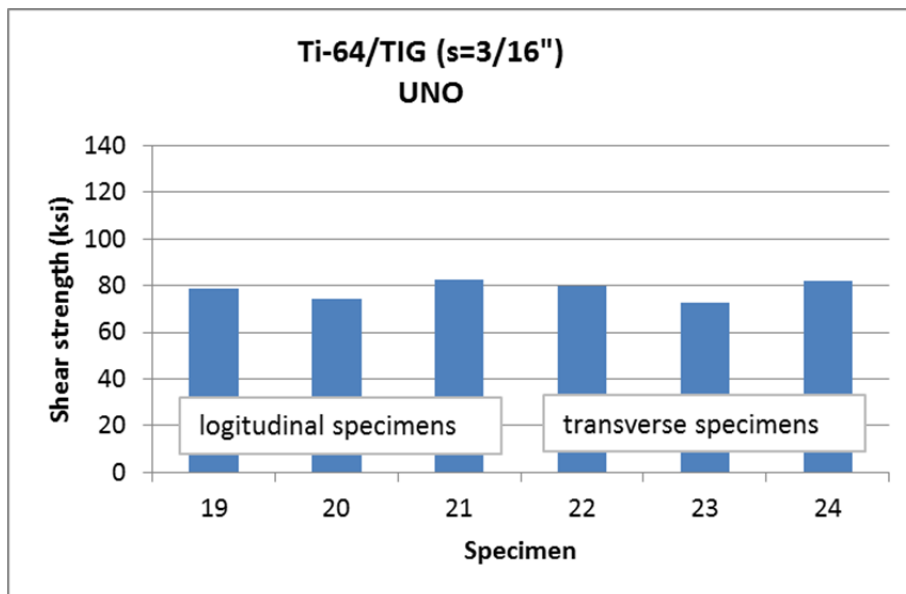


Figure 43 Typical smaller values for 3/16" welds

The previous charts serve to showcase the irregularity of the larger welds having lower Shear Strength values than the larger ones; this is believed to be due to a higher concentration of imperfections in larger welds. The following images show typical close-ups at the root of the welds; they confirm the trend that larger welds contain imperfections more often and larger

than smaller welds (Figures 44 & 45). The area within the weld profile from which these images come from is illustrated in Figure 39.

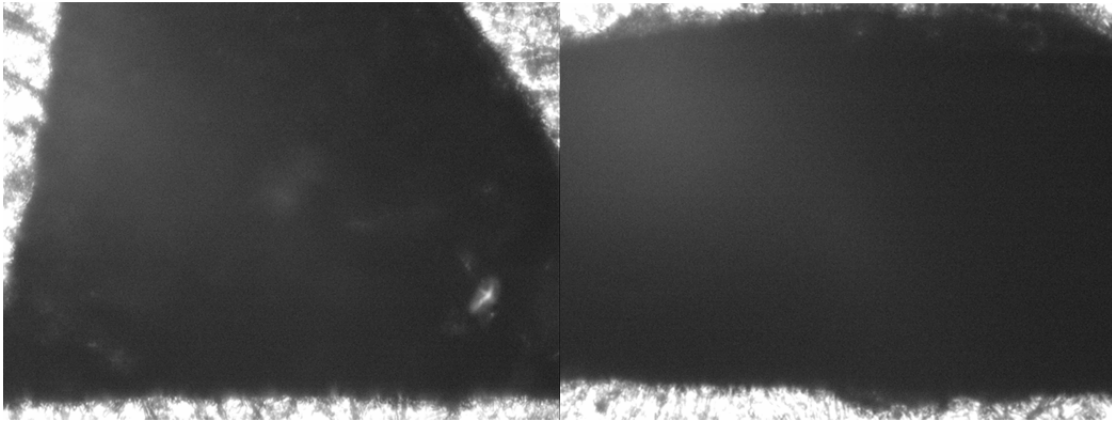


Figure 44 Typical profiles at the root of larger 3/16" welds

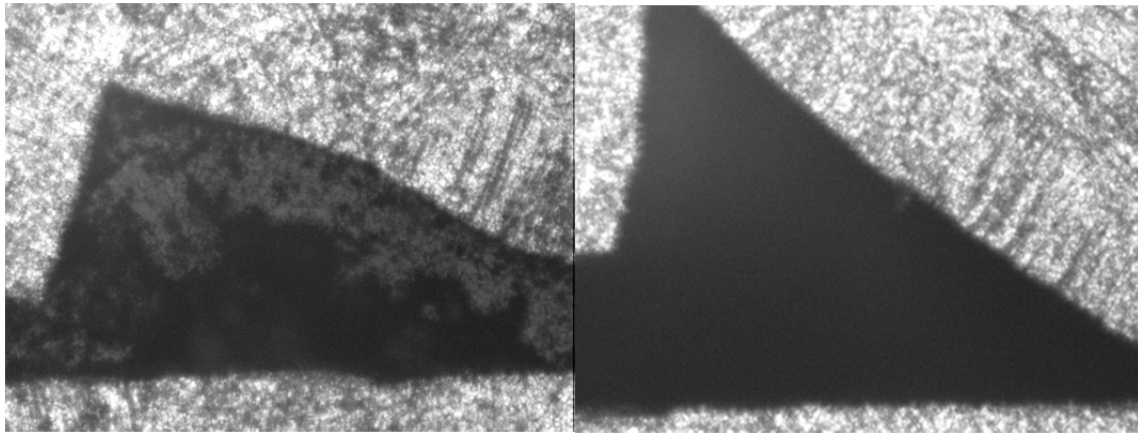


Figure 45 Better penetration is visible in these smaller 1/8" welds

Taking into account those irregularities, those specimens deemed defective are set aside as we now look to compare the correlation between Longitudinal and Transverse Shear Strength values with the improved formulas. Figure 46 & 47 show the typical comparison between the correlation achieved by AWS and that obtained by UNO when both are using data measured before the specimens are tested.

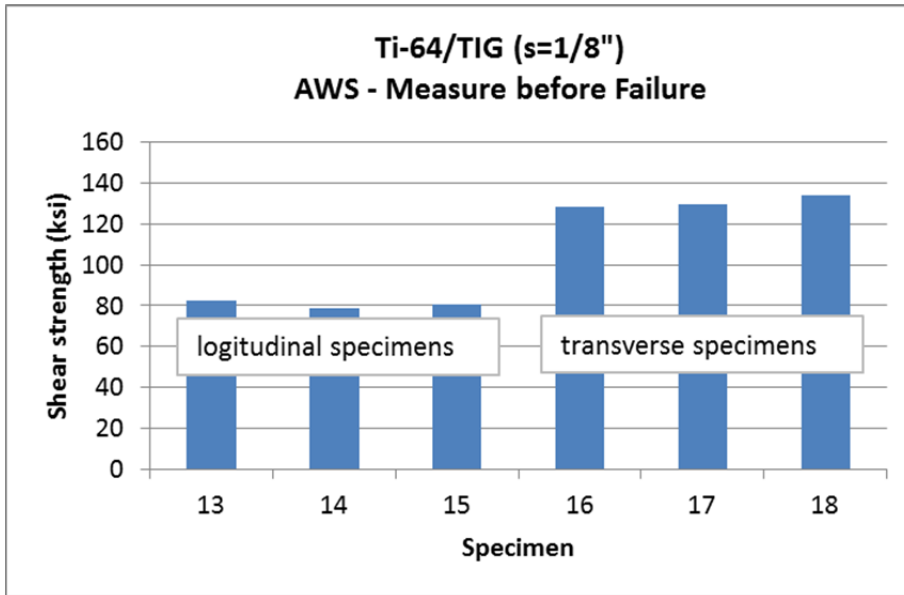


Figure 46 A typical display of the Shear Strength values achieved by the AWS formula and the lack of correlation between the specimens

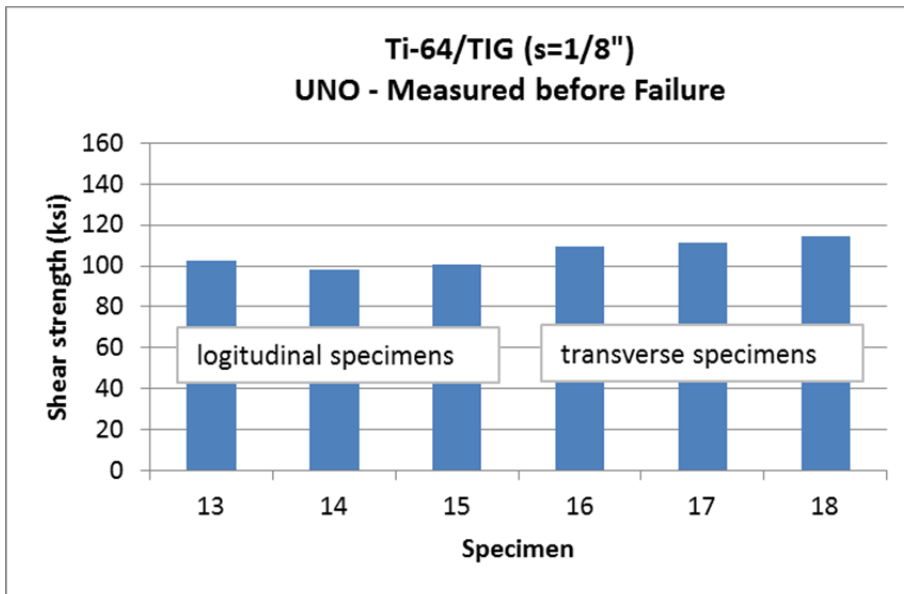


Figure 47 A typical display of how UNO Shear Strength results do correlate between Longitudinal and Transverse specimens

The imperfections that cause these issues are illustrated in the photographs shown next. Figures 48 - 51 display the typical outcome of a test conducted with flawed specimen.

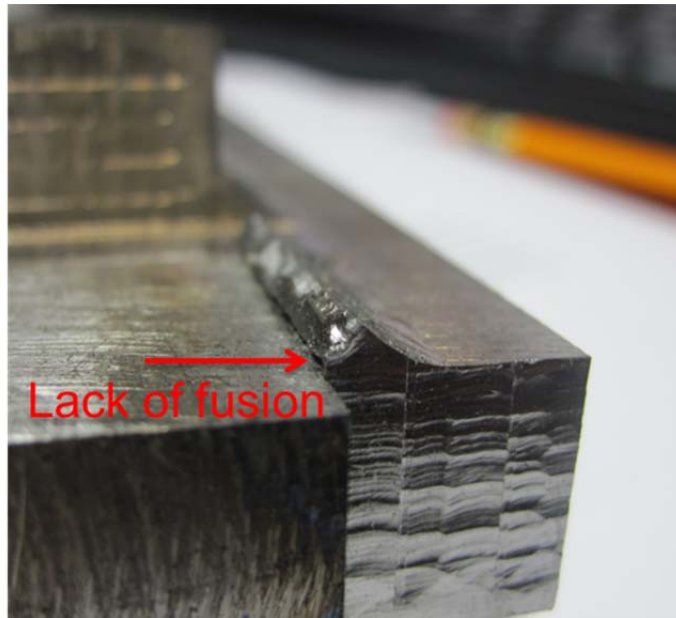


Figure 48 Lack of fusion is clearly visible in this weld after fracture has occurred

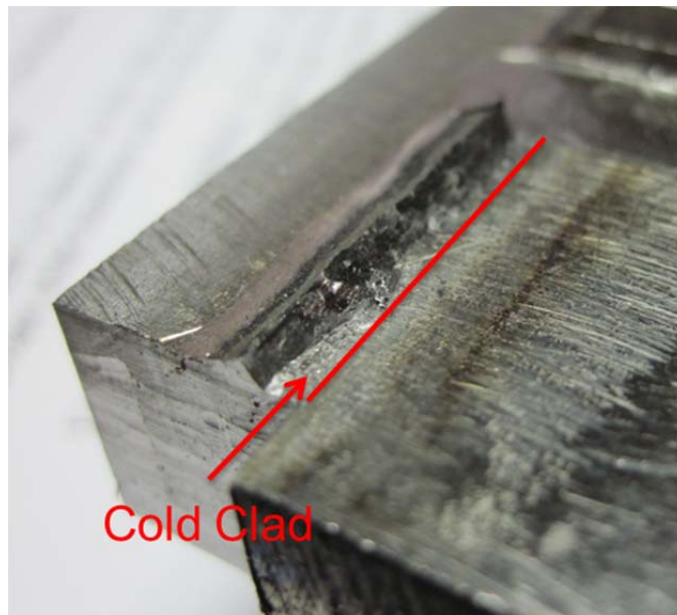


Figure 49 Cold clad is shown in this weld as the base plate separated entirely from the weld material



Figure 50 Another example of the recurrent lack of penetration

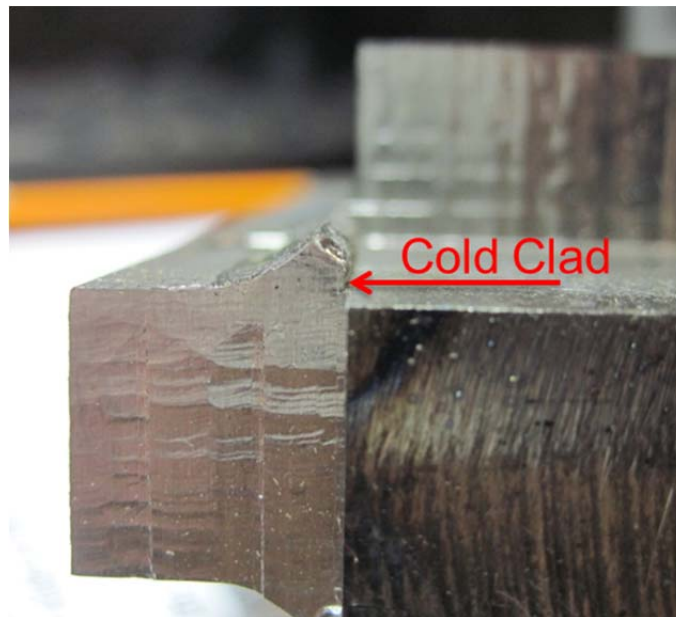


Figure 51 An almost vertical disconnection shows a typical cold clad

Adding another level of complexity to the study, the results are compared using the data obtained after the specimens were tested to failure. Figure 52 shows how AWS values correlate even worse when the real values for leg sizes are used; this after-breaking values take into account all imperfections, making them more accurate compared to the values measured before fracture. Figure 53 shows how UNO's equations continue to yield values for Shear Strength that correlate much better between Longitudinal and Transverse specimens.

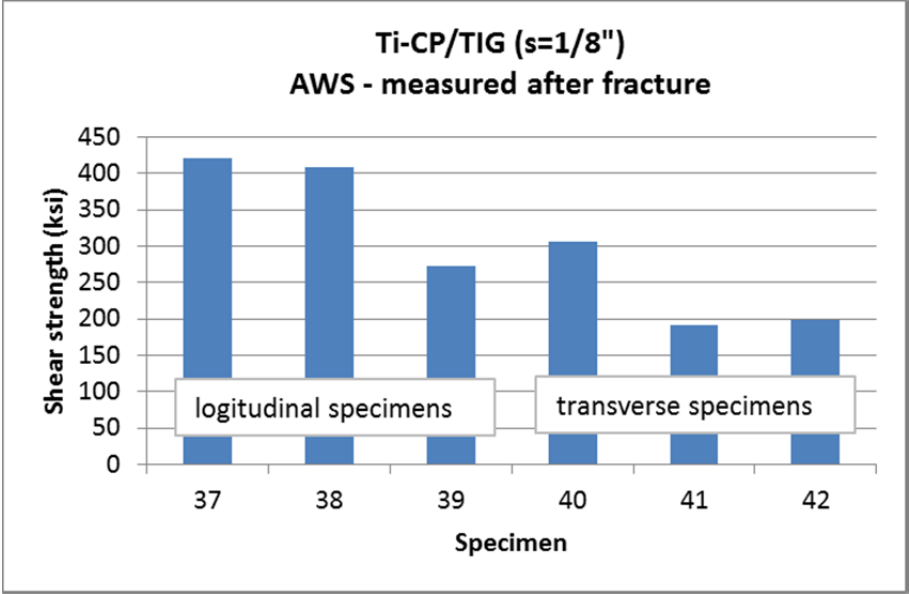


Figure 52 AWS results using after fracture measurements do not correlate between specimens

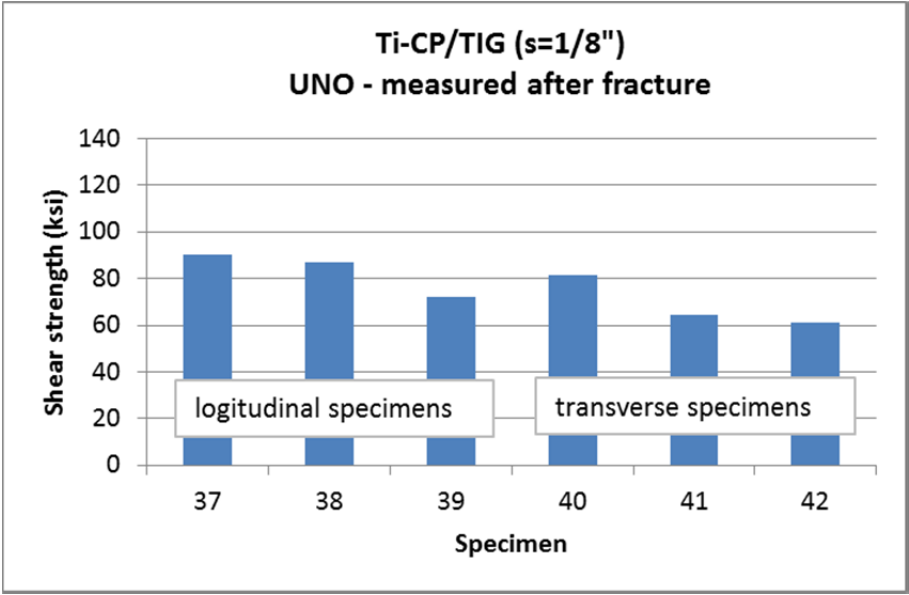


Figure 53 Shear Strength correlation between Longitudinal and Transverse specimens is achieved with UNO's equations

VIII. CONCLUSIONS

A. Better Shear Strength correlation

The equations provided and used by the UNO team show the best correlation for Shear Strength between Longitudinal and Transverse specimens whether the data is acquired before or after the testing is conducted. AWS's values do not correlate in either case, yet they show a trend to worsen when using the more realistic data measured after testing was conducted.

B. Low Shear Strength values for TIG

TIG welded specimens show a trend to have lower Shear Strength values than their MIG counterpart with the same leg size target and materials. Partially, this trend can be explained by an observed higher concentration of larger imperfections within TIG welds than those found in MIG welded specimens. Lack of penetration and cold clads are among the issues that repeat themselves more often in TIG welding than in MIG processes. The issue was improved approximately by 20% by using weld leg sizes measured after fracture; this improvement does not entirely get rid of the discrepancies found between MIG and TIG specimen's shear strength and therefore, further research ought to be conducted in other areas such as microstructures and increased detail in the differences between the two weld processes must be recorded to reach a better explanation of why the discrepancy still persists.

C. Larger welds have lower Shear Strength than smaller welds

This issue was also shown to be a consequence of weld imperfections being most common in larger welds than they are in smaller ones. This issue also serves to empower the call for smaller welds in industry that these projects all attempt to achieve; lowering weld sizes will reduce the stresses and distortions found in welded structures, and while still being strong enough for the necessary applications, this will also reduce weight and manufacturing costs.

WORKS CITED

- [1] AWS B4.0: 2007 Standard Methods for Mechanical Testing of Welds
- [2] ASTM E8
- [3] Krumpfen Jr., R.P.; Jordan, C.R.. Reduced fillet weld sizes for naval ships. *Welding Journal*, 1984, 63(4): 34~41
- [4] Nie, C.; Dong, P.. Traction Stress Based Shear Strength Definition of Fillet Welds. Pending Publishing.
- [5] ATI 38-644 Beta Titanium Alloy. Technical Data Sheet.
- [6] Oxford Alloys, Inc. Certified Material Test Report for Grade 5 Titanium.
- [7] R. W. McClellan. Evaluation of the fillet weld shear strength of flux cored arc welding electrodes. NSRP 0320, paper No. 5B-1, 1990.
- [8] S. Timoshenko. Theory of elasticity. McGraw-Hill Book Co., 1951
- [9] Ben Kato, Koji Morita. Strength of transverse fillet welded joints. *Welding Journal*, 1974, 53(2): 59~64
- [10] G. Kamtekar. A new analysis of the strength of some simple fillet welded connections. *Journal of Constructional Steel Research*, 1982, 2(2): 33~45
- [11] Dong, P , Hong, JK et al, "The Master S-N Curve Method: *An Implementation For Fatigue Evaluation Of Welded Components in the 2007 ASME B&PV Code, Section VIII, Division 2 and API 579-1/ASME FFS-1,*" WRC Bulletin, No. 523, December, 2010, New York, New York.
- [12] Similar Triangles. [http:// www.mathopenref.com/similartriangles.html](http://www.mathopenref.com/similartriangles.html)

VITA

Erasto Fernandez was born in Caracas, Venezuela to Erasto Fernandez and Claudia Zapata. He received his undergraduate degree in Ocean Engineering at Florida Atlantic University in May 2010. He became a Citizen of the United States of America in 2011. He will be receiving his graduate degree at the University of New Orleans in May 2012. He has worked for Dr. Pingsha Dong as a graduate assistant in the School of Naval Architecture and Marine Engineering for over a year now and will continue to do so as he pursues his PhD in the same College and concentration.